Since January 2020 Elsevier has created a COVID-19 resource centre with free information in English and Mandarin on the novel coronavirus COVID-19. The COVID-19 resource centre is hosted on Elsevier Connect, the company's public news and information website.

Tetrahedron 76 (2020) 131373

Contents lists available at ScienceDirect

Tetrahedron

journal homepage: www.elsevier.com/locate/tet

Assistance of DFT calculations on the design and rationalization of active pharmaceutical ingredients synthesis – Michael addition-isomerization steps in Oseltamivir synthesis

Pedro Paulo Santos*, Luís F. Veiros

Centro de Química Estrutural and Departamento de Engenharia Química, Instituto Superior Técnico, Universidade de Lisboa, Av Rovisco Pais, 1049-001, Lisboa, Portugal

ARTICLE INFO

Article history:
Received 12 March 2020
Received in revised form
27 June 2020
Accepted 30 June 2020
Available online 6 July 2020

Keywords:
DFT calculations
Stereoselective synthesis
Oseltamivir
Michael addition
Tamiflu
Active pharmaceutical ingredients
Thermodynamic control

ABSTRACT

The Michael addition step and the following C5 isomerization in Hayashi's synthesis of Oseltamivir was studied by means of a DFT mechanistic study. These steps are crucial for the viability of the process where the formation of a single stereoisomer is required. The results indicate that the addition reaction is under thermodynamic and not kinetic control and that the key factor determining the reaction stereoselectivity are the stereochemical constraints imposed by all substituents in the cyclohexane ring. The DFT results indicate that cyclohexylthiol should behave similarly to *p*-toluylthiol, the one actually employed, and *tert*-butylthiol should increase the ratio between isomers favoring the desired *S* configuration of the C5 atom. This work shows that DFT studies can be useful in the selection of a reactant to improve stereoselectivity of a chemical step.

1. Introduction

Oseltamivir (Fig. 1) was invented by Gilead in 1995 [1] during a program of search for orally active inhibitors of Neuraminidase for the treatment and prevention of influenza viral infections. The active pharmaceutical ingredient (API) was launched as Tamiflu® in 1999, being one of the most potent antiviral drugs on the market and listed since 2009 as an essential medicine by the World Health Organization [2].

The API is a fairly small but complex chiral molecule with three asymmetric centres having a 3,4,5-trisubstituted cyclohex-1-enecarboxylate ester core structure. The discovery synthesis of Oseltamivir started from natural (−)-Shikimic acid or (−)-Quinic acid and resemblance between the three structures is quite evident (Fig. 1). The carbocyclic system is already present, the double bond is at the correct position and all carbon atoms of the cycle are at the right oxidation state i.e. no oxidation or reduction steps are required to produce Oseltamivir from shikimic acid. It is predicted that a total synthesis of Oseltamivir would hardly compete with a semisynthetic process.

Oseltamivir became worldwide famous when it was appointed as one of the few drugs available active against the avian H5N1 influenza virus as well as the H1N1 swine influenza strain [3]. Oseltamivir is currently being tested against the new coronavirus (2019-nCoV) [4]. The fear of a disastrous pandemic event back in 2012 triggered an increasing demand for stocking huge amounts of Oseltamivir and the worldwide annual production of shikimic acid was short of the material needed [5]. At the time, the emergence of new Oseltamivir synthetic routes not based on the natural sources became a priority. Both industrial and academic chemists undertook a huge effort to develop synthetic alternatives for the synthesis of Oseltamivir. More than 60 syntheses, using very different strategies along with several variations were published, most of them were reviewed [5,6]. Many of these can be excluded from consideration for application at an industrial level because of low yields, reduced throughput, chromatographic purifications, oily intermediates and inherent safety hazards. Others may warrant further investigation and one of the most promising routes was first disclosed and patent protected by Hayashi [7] and was further optimized at a gram scale (Scheme 1 [8]).

* Corresponding author.
E-mail address: pepesantos@tecnico.ulisboa.pt (P.P. Santos).

https://doi.org/10.1016/j.tet.2020.131373
0040-4020/

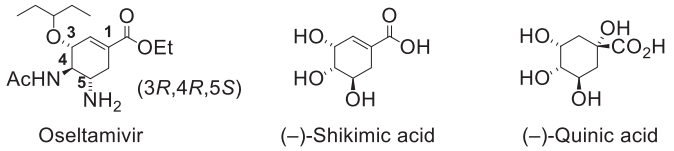

Fig. 1. Structure of Oseltamivir, (−)-Shikimic acid and (−)-Quinic acid.

This short high yielding, simple to operate outstanding synthesis was clearly designed to be industrialized: catalyst for asymmetric synthesis easily accessible and relatively inexpensive, one-pot procedures for sequential reactions, isolable crystalline intermediate serves as a clean-up point and viability proven at gram scale. However, there are issues associated with availability of starting materials, odor of *p*-toluenethiol and the use of azide chemistry in a Curtius rearrangement to convert the *tert*-butyl ester into the primary amine. An efficient, practical, and safe microflow reaction of the Curtius rearrangement using trimethylsilyl azide as an azide source was developed [9]. The use OsO_4 and CH_3NO_2 in the production of the starting materials for the synthesis is also of concern.

Key reactions on this route are clearly the ones where the configuration of the chiral centres of Oseltamivir is set. The first organocatalyzed Michael addition establishes the configuration of the C3 and C4 carbons of Oseltamivir and was extensively studied [8b] (Scheme 2, step 1). The second stage of the cycle build-up involves domino reactions under basic reaction conditions: a Michael addition with vinylphosphonate (ethyl 2-(diethoxyphosphoryl)acrylate) followed by an intramolecular Horner–Wadsworth–Emmons reaction to form the cyclohexene carboxylate ester (Scheme 2, step 2).

This domino sequence produces directly the core cyclohexene ring of Oseltamivir, despite the *R* configuration at the C5 carbon ring atom of the main isomer formed. This isomers mixture was unsuitable for industrial production as chromatographic methods cannot be applied at large scale batches and taking into account the isomers proportion, a maximum yield of 12% [8a,b] for the intended 5*S* isomer is very unsatisfactory, ruining the utility of the synthesis. More, the mixture of the C5 epimers is described as inseparable by chromatography [8b].

Acid- or base-mediated isomerization of the 5*R* to the 5*S* epimer was partially successful giving in the most favorable cases an almost equimolar mixture of the two compounds [8b]. The projected yield of the 5*S* intermediate was upgraded to 35% [8a] but the problem of the isomers separation still remained to be solved. A breakthrough was found by adding *p*-toluenothiol to the basic mixture of the epimers in the reaction mixture to promote a Michael addition reaction and it turned possible to isolate a sole 5*S* cyclohexane thiol-addition product as a crystalline solid in 70% yield from the starting nitro olefin. That critical base-catalyzed Michael addition-isomerization step sets the configuration at C5 carbon and allows the isolation of a sole isomer with five chiral carbon centres at the saturated carbon cycle. At this stage of the

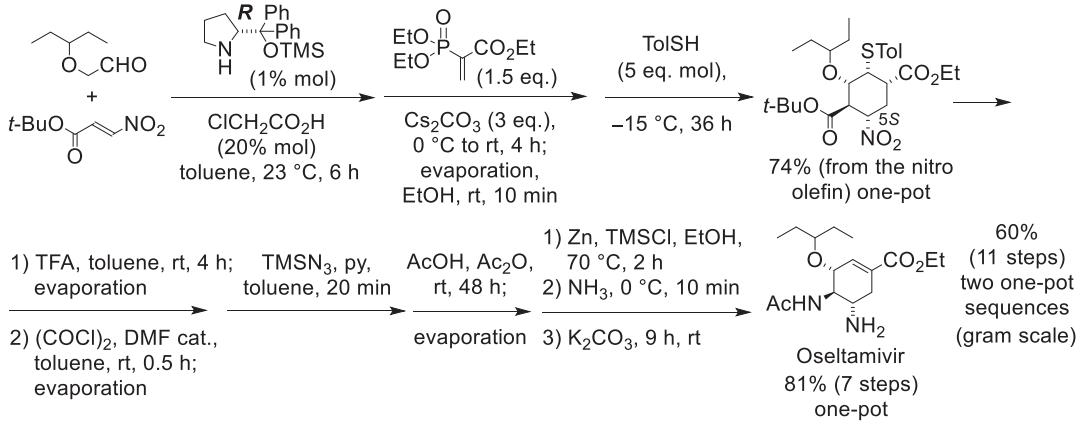

Scheme 1. One of the most promising non-shikimic acid-based routes to produce Oseltamivir.

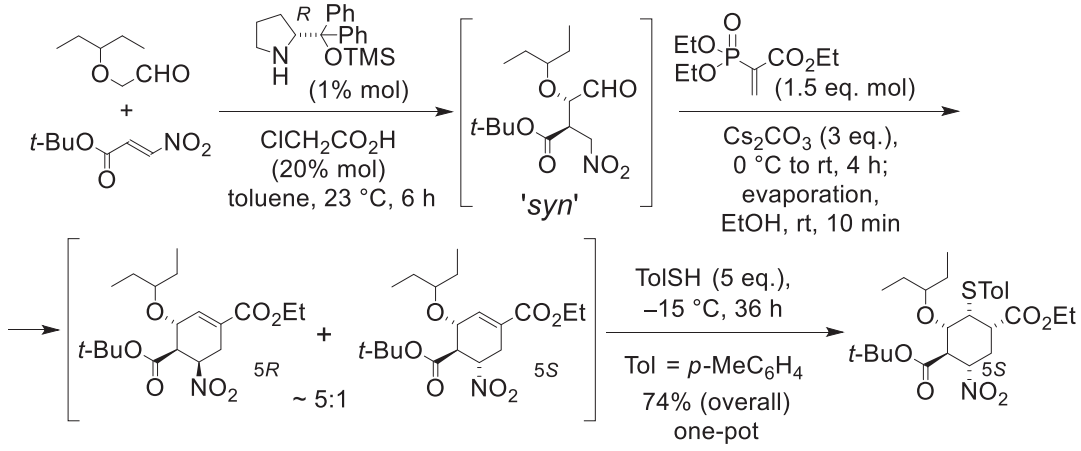

Scheme 2. Build-up of the cyclohexane ring by the Hayashi method.

synthetic route the presence of carbonate is crucial, acting as a base in two different ways, promoting both reactions that do not occur in its absence [8]. However, the stereochemical features involved in this reaction step were not fully investigated.

Having the configuration of the various carbon centres established in the Michael addition product, Oseltamivir was obtained by conversion of the *tert*-butoxycarbonyl group into an acetylamino moiety, reduction of the nitro group into an amine and promoting a retro-Michael step in basic conditions to reveal the unsaturated cyclohexene ring (Scheme 1). The ingenious introduction of the Michael addition step and its reverse reaction was able to allow a favorable isomerization at the C5 of the cyclohexane intermediate. This strategy may be applied for other synthetic procedures.

In this work we describe a DFT mechanistic study of the crucial Michael addition-isomerization step aiming the understanding of the factors determining its high stereoselectivity, vital for the success of the entire API synthetic procedure. The influence of the size and shape of the thiol substituent on the isomerization of the C5 carbon is discussed.

2. Results and discussion

When the original synthetic plan was devised, it was predicted that fully isomerization of the C5 carbon atom to the supposed more stable 5*S* epimer, with the nitro group at an equatorial position, should be easy. As simple base mediated isomerization of the C5 carbon of the cyclohexene was only partially successful, a Michael addition of thiolate ($TolS^-$) to the cyclohexene ring was set as a key step in the synthesis of the anti-influenza active principle Oseltamivir, in order to obtain an *S* configuration in the C5 carbon atom. In fact, the high stereoselectivity of that reaction allows the effective formation of only one of eight possible diastereomers. While the configuration of C3 and C4, bearing substituents Et_2CHO and COO^tBu, respectively, is pre-established in the reactant and will not change along the reaction, each one of the remaining three substituents in the product, COOEt, STol and NO_2, could adopt one of two possible orientations and lead to two configurations of each C1, C2 and C5 carbon atoms. The mechanism of that reaction was addressed by means of DFT calculations [10] aiming the understanding the observed stereoselectivity.

The structure calculated for the product of the reaction is represented in Fig. 2. The most stable chair conformation of the ring has all the substituents in equatorial positions except the thiolate. In fact, the bulkiest substituents, Et_2CHO and COO^tBu, dictate the stability of the ring conformation. These were already present in the reactant cyclohexene and their orientation will determine the most stable conformation of the cyclohexane ring in all diastereomers.

The stability of all the isomers that result from two possible configurations of C1, C2 and C5, that is, the position occupied by COOEt, STol and NO_2, was evaluated through the optimization of the corresponding geometry and the results are schematically represented in Fig. 3. Their structures are depicted in Fig. S1 (Sup. Information).

The stability of all isomers is within $\Delta G = 5.3$ kcal/mol but the product observed (**A**) is the most stable of all forms, despite the fact that the thiolate group occupies an axial position. In fact, the size and number of all the substituents around the ring make the isomer with all groups in equatorial position (**F**) only the second most stable form, 2.2 kcal/mol above **A**. This result indicates that the

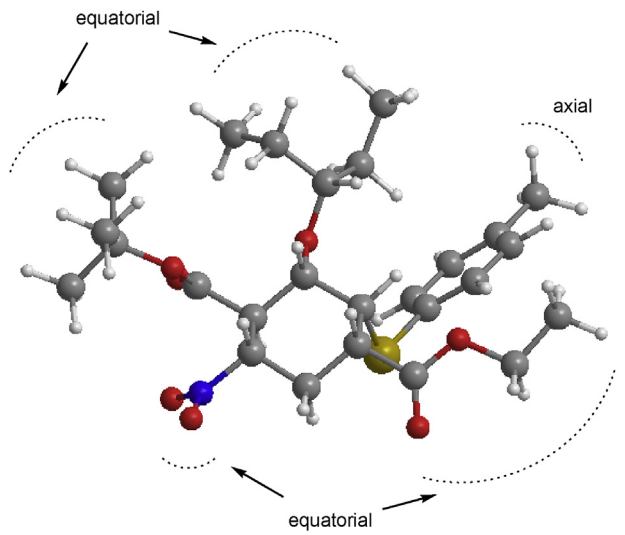

Fig. 2. Optimized structure obtained for the product of the Michael addition (**A**).

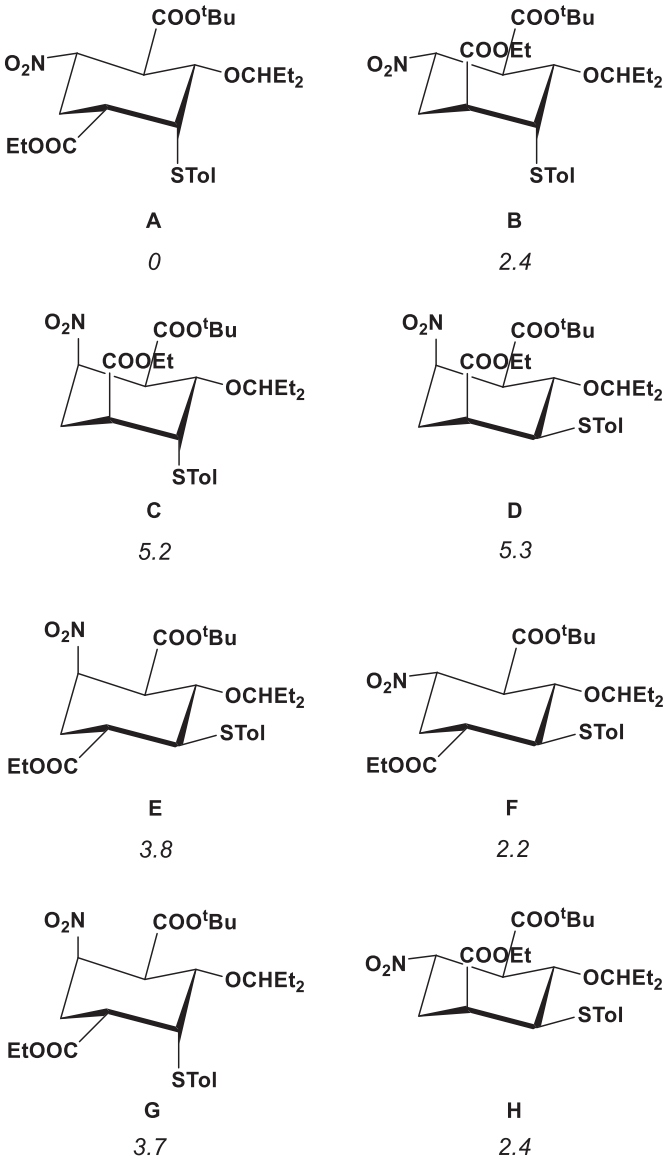

Fig. 3. Comparison between the stability of all calculated diastereomers resulting from different configurations of C1, C2 and C5 in the cyclohexane ring. Free energy values (italics) in kcal/mol, relative to the product, **A**.

isomer experimentally obtained corresponds to the thermodynamic product of the reaction.

The free energy profiles for the addition of thiolate, $TolS^-$ [11], to the cyclohexene ring are represented in Scheme 3. From our calculations, two possible approaches of the nucleophile were found possible and compared. In one case, $TolS^-$ attack occurs on the side opposite to most ring substituents (all except COO^tBu), going through transition state **TS_{12}** and leading to product **F**, after protonation. On the other orientation, the nucleophile attack happens at the side of the ring most occupied by other groups. In this case, the reaction goes through transition state **TS_{34}** and the final product is **A**, that is, the one experimentally observed.

Although **A** is the most stable of the two products, as discussed above, the corresponding reaction involves the highest barrier, with **TS_{34}** 3.9 kcal/mol less stable than **TS_{12}**. In **TS_{12}**, the ring conformation tends to the twist-boat that is fully present in the resulting intermediate, **2**. This will be protonated yielding product **F** after the rearrangement of the ring to a chair conformation that brings all substituents, including STol, to equatorial positions. Along that path, $TolS^-$ reaches the cyclohexene ring from the side of C_6-ring that is most uncrowded from the stereochemical point of view (see Fig. 4). Conversely, in the case of **TS_{34}** the ring is moving to a chair conformation, completely formed in intermediate **4**. This conformation is maintained after protonation and in the final product, **A**. One major difference between the two paths is that, in the second, the nucleophile has to approach the ring from the same side were most substituents lie. This is particularly important in the case of the $OCHEt_2$ group since this is located on the C-atom adjacent to the one where the addition occurs (Fig. 4). The consequence is a destabilization of transition state **TS_{34}** and a higher energy barrier. This is reflected in the geometry of the two transition states, with a closer S–C distance in the case of **TS_{12}**, compared with the one in **TS_{34}**. This means that once the transition state is reached and the C–S bond is about to be formed the two reactants are closer in the

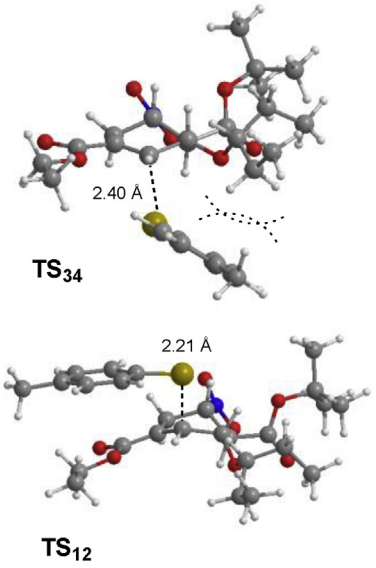

Fig. 4. Comparison between transition states **TS_{12}** and **TS_{34}**.

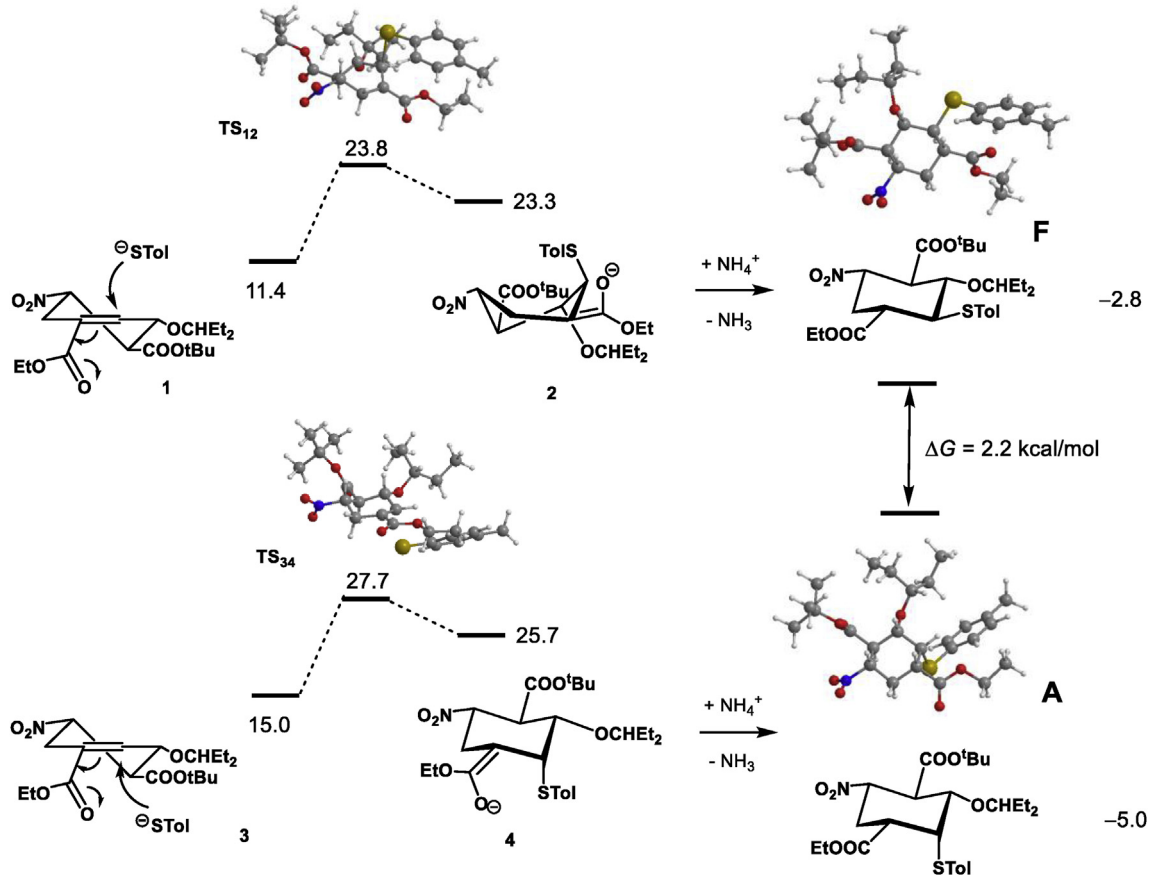

Scheme 3. Free energy profiles calculated for the step of thiolate attack of the synthesis of Oseltamivir. Nucleophile attack on the two sides of the cyclohexene ring was considered and free energy values (kcal/mol) are relative to the separated reagents: substrate + TolSH + NH_3 (as model for the base catalyst).

case of $\mathbf{TS_{12}}$, resulting in a stronger interaction and a more stable transition state.

Thus, the results indicate that although the product observed, **A**, is the most stable one its formation requires a higher energy barrier, that is, the reaction is under thermodynamic and not under kinetic control. Moreover, the major difference between the two possible reaction paths is caused by stereochemical repulsion between the incoming nucleophile and the substituents in the cyclohexene ring.

The observed thermodynamic control can be explained by the reversibility of the Michael addition step. This assumption is supported by the fact that the last step of Hayashi's route is the removal of the thiolate to form Oseltamivir which follows an E1cB mechanism with the assistance of sodium carbonate as base. This final elimination step that is in fact the reverse of the Michael addition step, uses same base and solvent as the Michael addition step but obviously different molar quantities of reactants to promote the desired reaction efficiently. Our calculations are in total agreement with the experimental results as the prolonged reaction times and excess of both nucleophile and base will help the equilibrium to be reached.

The profiles in Scheme 3 correspond to thiolate attack on the cyclohexene reactant with a *S* configuration in the C5 atom. The mechanism of the Michael addition reaction was also addressed starting from the cyclohexene reactant with opposite configuration in C5 (*R*), maintaining the configuration of all the other C-atoms. The free energy profile obtained is presented as Supporting Information (Fig. S4). The calculated energy barriers (29–30 kcal/mol) indicate processes clearly less facile than the ones obtained for the reaction with the *S* isomers.

In order to validate the conclusions above, the same reaction mechanism was calculated with a cyclohexene ring without any substituents apart front the acceptor COOEt group on the C=C double bond. The free energy profiles obtained are represented in Scheme 4.

The energy profiles in Scheme 4 show that the most stable product (**J**) is the one with both substituents in equatorial positions, as expected from simple stereochemical reasoning. In fact, this molecule is more stable by $\Delta G = 2.0$ kcal/mol than the alternative one (**I**) where the thiolate occupies an axial position while the ester group remains equatorial. Interestingly, the energy barriers are reversed with respect to that stability order. That is, the product that is formed through a lower energy barrier is the less stable one, **I**. Thus, when the thiolate approaches the substrate by one side of ring the resulting transition state ($\mathbf{TS_{56}}$) presents a chair-like conformation of the ring, a conformation that is maintained in the ensuing intermediate, **6**, and in the product yielded after protonation, **I**. On the other hand, if the relative position of the two reagents is the opposite, i.e., if the thiolate attacks on the other side of the cyclohexene ring, the transition state ($\mathbf{TS_{78}}$) has a twist-boat conformation of the ring, also present on the following intermediate, **8**. Here, after protonation and rearrangement of the ring to a chair conformation, there is formation of the product with the two equatorial substituents, **J**. Overall, the second barrier is higher than the first one by 2.3 kcal/mol. Therefore, the major factor controlling the reaction barrier is the conformation of the C_6-ring in the transition state, while stereochemical repulsion dictates the product stability, in good accordance to what is generally known [12].

In summary, without bulky substituents the kinetic product is the one that follows axial attack of the nucleophile and the most stable product is the one with the substituents in equatorial positions, contrarily to what was found in the case of the substituted

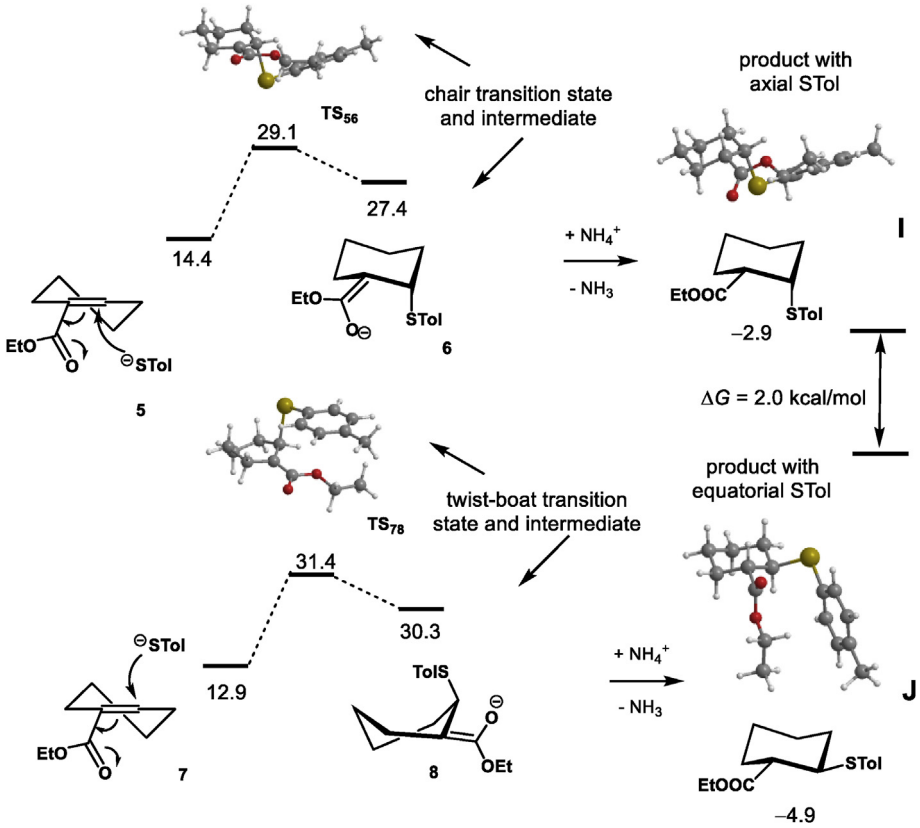

Scheme 4. Free energy profiles calculated for the thiolate attack on the two sides of a cyclohexene ring without substituents (ethylcyclohex-1-enecarboxylate). Free energy values (kcal/mol) are relative to the separated reagents: substrate + TolSH + NH_3 (as model for the base catalyst).

cyclohexene intermediate in the synthesis of Oseltamivir. This provides strong support to the conclusion that the outcome of that reaction is due to the presence of bulky substituents in the C_6-ring.

The final configuration on the second C-atom of the double bond (C1) is accomplished after protonation of the species that results from the attack of the thiolate, intermediate **4** in the profile Scheme 3. The most stable isomer is obtained with the COOEt group occupying an equatorial position, as expected from stereochemical reasons. In fact, this diastereomer (**A**) is more stable than the one with the alternative configuration in C1 (**B**) by $\Delta G = 2.4$ kcal/mol (see Fig. 3 and Fig. S2).

The third and last C-configuration that is defined in the Michael addition-isomerization step of the synthesis of Oseltamivir is on C5, the carbon atom bearing the NO_2 group. Again, the preferred configuration (*S*) corresponds to the NO_2 in the equatorial position of the reaction product, **A**. The alternative isomer with the substituent in the axial position (**G**) is less stable than **A** by $\Delta G = 3.7$ kcal/mol (Fig. 3 and Fig. S2). This value is significantly higher than the one obtained for the stability difference between the two corresponding isomers in the cyclohexene reactant with the C5 atom in *R* or in *S* configuration ($\Delta G = 1.6$ kcal/mol, see Fig. S3 in the Supporting Information). This corroborates the experimental data and, in fact, the need for the Michael addition step in the synthesis. In the case of the reactant, both enantiomers are present in practically equal amount after long treatment with base [8]. Conversely, the cyclohexane ring present in the product, being more demanding from the stereochemical point of view, increases the stability difference between stereoisomers and allows the preferential formation of the intended stereoisomer.

The C5–H bond in **A** is rather acidic due to the neighborhood of NO_2, as clearly demonstrated for the cyclohexene precursor were the *R*–*S* isomerization in C5 is observed under mild conditions in basic medium, for example with triethylamine at 23 °C along 4 h [8]. Thus, equilibration between C5 *R* and *S* isomers occurs certainly in the reactant but is also possible in the product, **A**, justifying the mechanistic study of the corresponding proton exchange. Ammonia was used as model for the base catalyst and the free energy profile obtained is depicted in Scheme 5.

The isomerization process starts with the pair of reactants, ammonia and the product **A**, represented by **K** in the profile. Here, NH_3 approaches **A** by the side of ring opposite to the one occupied by most substituents, and the pair of molecules is stabilized by a moderate N–H interaction (d = 2.31 Å). The reaction proceeds with C–H proton abstraction and formation of the ammonium cation, through transition state $\mathbf{TS_{KL}}$. The corresponding barrier is only 12.7 kcal/mol and, thus, easily overcome in the reaction conditions. In the transition state the process is well advanced with a C–H elongated to 1.40 Å and the incipient N–H bond almost formed (d = 1.31 Å). The resulting intermediate, **L**, is stabilized by a strong H-bond established between the ammonium ion and the O-atom of the NO_2 group ($d_{H-O} = 1.52$ Å). From **L** to **L′**, there is a change in the relative position of the two species with the NH_4^+ ion moving from one side of the C_6-ring to the other. Intermediate **L′** is also stabilized by a H-bond between NH_4^+ and the deprotonated product, similarly to what happens with **L** ($d_{H-O} = 1.53$ Å). The final step in the mechanism is re-protonation of C5. This occurs trough transition state $\mathbf{TS_{L'M}}$, in a way that parallels what was discussed for $\mathbf{TS_{KL}}$ ($d_{N-H} = 1.30$ Å and $d_{C-H} = 1.40$ Å). The final species (**M**) corresponds to the pair of molecules, isomer **G** plus ammonia, and presents the NO_2 group in an axial position and an *R* configuration on the C5-atom, naturally. The overall barrier is accessible (16.0 kcal/mol, $\mathbf{TS_{L'M}}$) and the overall process is endergonic by $\Delta G = 3.9$ kcal/mol, reflecting the stability difference between isomers.

In summary, simple acid-base reactions allow the exchange between the isomers with *R* and *S* configuration in the C5-atom, both in the cyclohexene reactant as well as in the product **A**. In the former the two isomers have similar stability, while in the product the stability difference increases and the *S* isomer becomes clearly the most stable and, thus, the one that is finally obtained. That stability difference is a consequence of the increased stereochemical constraints of the cyclohexene ring, compared with the cyclohexane and, thus, will depend on the bulkiness of the thiolate

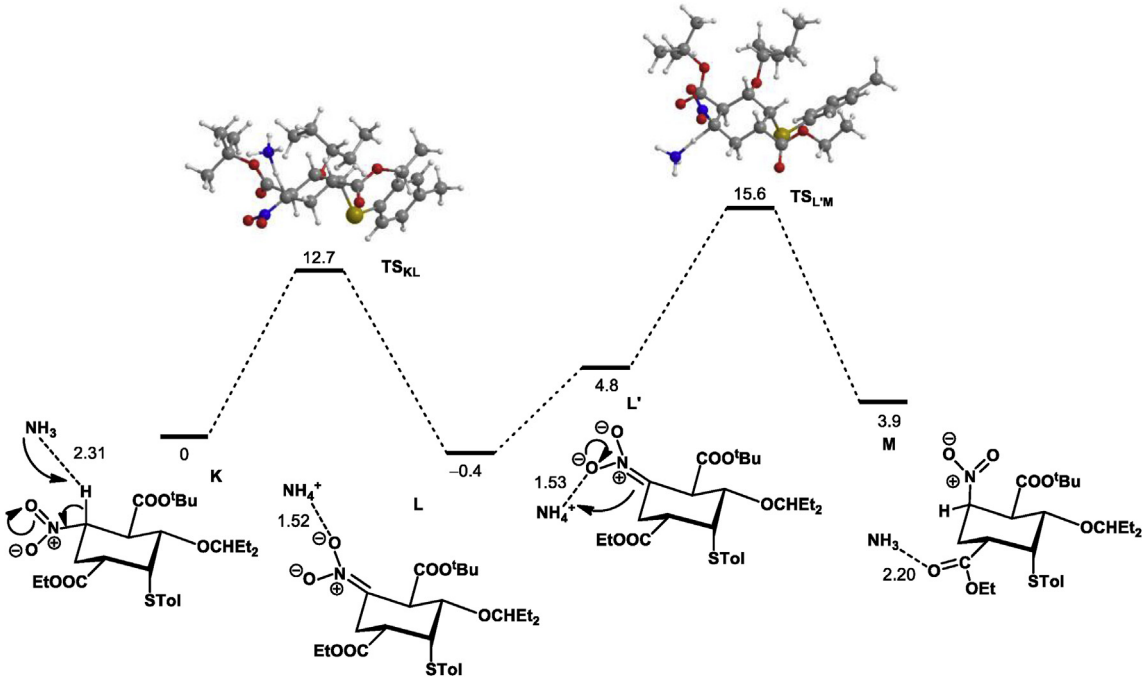

Scheme 5. Free energy profile calculated for *R*–*S* isomerization in the C5 position of the product, **A**, catalyzed by ammonia. Free energy values (kcal/mol) are relative to the pair of reagents (**K**). Distances in Å.

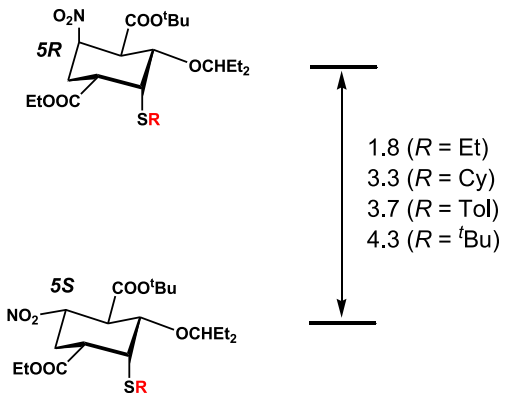

Fig. 5. Stability difference (Δ*G* in kcal/mol) for the two isomers with different C5 configuration as a function of the thiolate substituent R.

employed in the Michael addition. This issue was also addressed in the calculations and the stability difference between the two isomers, with *5R* or *5S* configuration is represented in Fig. 5 for selected thiolate substituents.

The results in Fig. 5 indicate that bulkier substituents increase the stability difference between the two isomers, as expected. The lowest value, 1.8 kcal/mol, is observed for R = ethyl, a value similar to one calculated for the cyclohexene precursor (see discussion above). Both the thiolate actually used (Tol), as well as cyclohexyl (Cy) have a comparable effect, showing an increase of the isomers stability difference relative to the one obtained with ethyl, 3.7 and 3.3 kcal/mol, respectively. The use of *tert*-butyl as thiolate substituent has the greater effect on the stability difference between C5 diastereomers, with a value of 4.3 kcal/mol. It should be noticed, however, that the greater bulkiness of *tert*-butylthiolate should also slow down the Michael addition with the corresponding loss of effectiveness.

The results above indicate that DFT calculations can be used to predict the stereochemical impact of the thiolate on the obtained epimer ratio and thus, could help planning the synthetic procedure. In the case studied, we could foretell that cyclohexylthiol is expected to have equal effect as toluylthiol, the one actually employed, while *tert*-butylthiol should provide a better ratio 5*S*/5*R* ratio, probably at the expenses of a slower addition.

3. Conclusions

The high stereoselectivity of the Michael addition step in the synthesis of Oseltamivir was addressed by a DFT mechanistic investigation. The results show that the isomer obtained is the most stable of all eight possible diastereomers despite the axial position occupied by the thiolate substituent in the molecule. In fact, the isomer with all substituents in equatorial positions would be the kinetic product of the reaction, but it is 2.2 kcal/mol less stable than the actual product. These results indicate that the reaction is under thermodynamic rather than kinetic control, and the reason could be traced to the stereochemical constraints imposed by the number and by the volume of the substituents around the C_6-cycle. It must be noticed that although the product presents the incoming nucleophile in an axial position as expected for an addition to a cyclohexene ring, the factors controlling the reaction outcome are different [12]. While in the case studied, that is the Michael addition step in the Oseltamivir synthesis, the product is the thermodynamic one and its stereochemistry is dictated by the stereochemical repulsion between the incoming nucleophile and the ring substituents, in the case of a less crowded cyclohexene the kinetic product is the one expected and the ring conformation in the transition state is the key factor in the reaction stereoselectivity.

An acid-base equilibrium allows the interchange between the isomers with different configurations of the C5-atom in both the reactant as well as in the product. However, in the case of the reactant both isomers have similar stability, while the *S* isomer becomes clearly more stable in the product due to the increased stereochemical constraints associated with the cyclohexane ring of the latter, when compared with the cyclohexene ring of the reactant. This is used to hold the C5 *S* configuration in the product and, in fact, constitutes the reason for the Michael addition step in the synthetic sequence of Oseltamivir. The stability difference between the two C5 diastereomers depends on the bulkiness of the thiol substituent, the bulkier the substituent, the higher the stability of the 5*S* form. However, bulkier thiolates should also be less efficient nucleophiles for the addition and, thus, a balance between those factors must exist. Toluylthiolate joints both conditions, being simultaneously bulky enough to differentiate the stability of the two isomers and allow the preferential formation of the intended one, while is still a good nucleophile allowing a feasible Michael addition step.

This work indicates that DFT studies may be useful in the design of the synthesis of active pharmaceutical ingredients through the elucidation of the stability of key intermediates or the unveiling of preferable reaction pathways.

3.1. Computational details

All calculations were performed using the Gaussian 09 software package [13], and the M06-2X functional, without symmetry constraints. That is a hybrid meta-GGA functional developed by Truhlar and Zhao [14], and it was shown to perform very well for main-group systems, providing a good description of long range effects such as van der Waals interactions or π-π stacking [15,16]. A standard 6-31G+(d,p) [17] basis set was used and solvent effects (ethanol) were considered by means of the Polarisable Continuum Model (PCM) initially devised by Tomasi and coworkers [18] with radii and non-electrostatic terms of the SMD solvation model, developed by Truhlar et al. [19] Transition state optimizations were performed with the Synchronous Transit-Guided Quasi-Newton Method (STQN) developed by Schlegel et al., [20] after a thorough search of the Potential Energy Surfaces (PES). Frequency calculations were performed to confirm the nature of the stationary points, yielding one imaginary frequency for the transition states and none for the minima. Each transition state was further confirmed by following its vibrational mode downhill on both sides, and obtaining the minima presented on the energy profiles. Electronic energies were converted to free energy at 298.15 K and 1 atm by using zero point energy and thermal energy corrections based on structural and vibration frequency data calculated at the same level.

Declaration of competing interest

The authors declare that they have no known competing financial interests or personal relationships that could have appeared to influence the work reported in this paper.

Acknowledgements

Centro de Química Estrutural acknowledges the financial support of Fundação para a Ciência e a Tecnologia (UIDB/00100/2020).

Appendix A. Supplementary data

Supplementary data to this article can be found online at https://doi.org/10.1016/j.tet.2020.131373.

References

[1] (a) S. Abrecht, P. Harrington, H. Iding, M. Karpf, R. Trussardi, B. Wirz, U. Zutter, CHIMIA Int. J. Chem. 58 (2004) 621–629;
(b) C.U. Kim, W. Lew, M.A. Williams, H. Liu, L. Zhang, S. Swaminathan, N. Bischofberger, M.S. Chen, D.B. Mendel, C.Y. Tai, W. Graeme Laver, R.C. Stevens, J. Am. Chem. Soc. 119 (1997) 681–690.(c) N. Bischofberger, C.U. Kim, L. Willard, L. Homgtao, M.A. Williams, (Gilead Sciences Inc.) U.S. Patent 5,763,483 A, June 09, 1998.

[2] World Health Organization, Model List of Essential Medicines, 21th List 2019, last update, 2019, august [online] Available, https://apps.who.int/iris/bitstream/handle/10665/325771/WHO-MVP-EMP-IAU-2019.06-eng.pdf?ua=1. (Accessed 17 February 2020).

[3] R.K. Saxena, P. Tripathi, G. Rawat, Eur. J. Clin. Microbiol. Infect. Dis. 31 (2012) 3265–3279.

[4] C. Huang, Y. Wang, X. Li, L. Ren, J. Zhao, Y. Hu, L. Zhang, G. Fan, J. Xu, X. Gu, Z. Cheng, T. Yu, J. Xia, Y. Wei, W. Wu, X. Xie, W. Yin, H. Li, M. Liu, Y. Xiao, H. Gao, L. Guo, J. Xie, G. Wang, R. Jiang, Z. Gao, Q. Jin, J. Wang, B. Cao, Lancet 395 (2020) 497–506.

[5] V. Farina, J.D. Brown, Angew. Chem. Int. Ed. 45 (2006) 7330–7334.

[6] (a) J. Magano, Chem. Rev. 109 (2009) 4398–4438;
(b) M. Shibasaki, M. Kanai, Eur. J. Org Chem. (2008) 1839–1850;
(c) M. Shibasaki, M. Kanai, K. Yamatsugu, Isr. J. Chem. 51 (2011) 316–328;
(d) P.P. Santos, W. Heggie, Retrosynthesis in the Manufacture of Generic Drugs, Selected Case Studies, Wiley-Blackwell, 2020, pp. 319–393 (in press).

[7] Hayashi Y., Ayashi Y., Ishikawa H., (Sumitomo chemical company) U.S. Patent 8,501,980 B2 Aug. 6, 2013, Eur. Pat. 2,301,911 B1 Aug. 19, 2015, prior date May, 30, 2008.

[8] (a) H. Ishikawa, T. Suzuki, H. Orita, T. Uchimaru, Y. Hayashi, Chem. Eur J. 16 (2010) 12616–12626;
(b) H. Ishikawa, T. Suzuki, Y. Hayashi, Angew. Chem. Int. Ed. 48 (2009) 1304–1307.

[9] H. Ishikawa, B. Bondzic, Y. Hayashi, Eur. J. Org Chem. 2011 (2011) 6020–6031.

[10] R.G. Parr, W. Yang, Density Functional Theory of Atoms and Molecules, Oxford University Press, New York, 1989.

[11] Since the reaction occurs with basic conditions (3 molar equivalents of Cs2CO3), thiolate (TolS-) should be promptly produced in the medium in a concentration high enough for the reaction to occur. The reaction does not occur in the absence of the base.

[12] J. Clayden, M. Greeves, S. Warren, P. Wothers, Organic Chemistry, Oxford University Press, 2005, pp. 858–859.

[13] Gaussian 09, Revision A.01 M.J. Frisch, G.W. Trucks, H.B. Schlegel, G.E. Scuseria, M.A. Robb, J.R. Cheeseman, G. Scalmani, V. Barone, B. Mennucci, G.A. Petersson, H. Nakatsuji, M. Caricato, X. Li, H.P. Hratchian, A.F. Izmaylov, J. Bloino, G. Zheng, J.L. Sonnenberg, M. Hada, M. Ehara, K. Toyota, R. Fukuda, J. Hasegawa, M. Ishida, T. Nakajima, Y. Honda, O. Kitao, H. Nakai, T. Vreven, J.A. Montgomery Jr., J.E. Peralta, F. Ogliaro, M. Bearpark, J.J. Heyd, E. Brothers, K.N. Kudin, V.N. Staroverov, R. Kobayashi, J. Normand, K. Raghavachari, A. Rendell, J.C. Burant, S.S. Iyengar, J. Tomasi, M. Cossi, N. Rega, J.M. Millam, M. Klene, J.E. Knox, J.B. Cross, V. Bakken, C. Adamo, J. Jaramillo, R. Gomperts, R.E. Stratmann, O. Yazyev, A.J. Austin, R. Cammi, C. Pomelli, J.W. Ochterski, R.L. Martin, K. Morokuma, V.G. Zakrzewski, G.A. Voth, P. Salvador, J.J. Dannenberg, S. Dapprich, A.D. Daniels, Ö. Farkas, J.B. Foresman, J.V. Ortiz, J. Cioslowski, D.J. Fox, Gaussian, Inc., Wallingford CT, 2009.

[14] Y. Zhao, D.G. Truhlar, Theor. Chem. Acc. 120 (2008) 215–241.

[15] Y. Zhao, D.G. Truhlar, Acc. Chem. Res. 41 (2008) 157–167.

[16] Y. Zhao, D.H. Truhlar, Chem. Phys. Lett. 502 (2011) 1–13.

[17] (a) R. Ditchfield, W.J. Hehre, J.A. Pople, J. Chem. Phys. 54 (1971) 724–728;
(b) W.J. Hehre, R. Ditchfield, J.A. Pople, J. Chem. Phys. 56 (1972) 2257–2261;
(c) P.C. Hariharan, J.A. Pople, Mol. Phys. 27 (1974) 209–214;
(d) M.S. Gordon, Chem. Phys. Lett. 76 (1980) 163–168;
(e) P.C. Hariharan, J.A. Pople, Theor. Chim. Acta 28 (1973) 213–222.

[18] (a) M.T. Cancès, B. Mennucci, J. Tomasi, J. Chem. Phys. 107 (1997) 3032–3041;
(b) M. Cossi, V. Barone, B. Mennucci, J. Tomasi, Chem. Phys. Lett. 286 (1998) 253–260;
(c) B. Mennucci, J. Tomasi, J. Chem. Phys. 106 (1997) 5151–5158;
(d) J. Tomasi, B. Mennucci, R. Cammi, Chem. Rev. 105 (2005) 2999–3094.

[19] A.V. Marenich, C.J. Cramer, D.G. Truhlar, J. Phys. Chem. B 113 (2009) 6378–6396.

[20] (a) C. Peng, P.Y. Ayala, H.B. Schlegel, M.J. Frisch, J. Comput. Chem. 17 (1996) 49–56;
(b) C. Peng, H.B. Schlegel, Isr. J. Chem. 33 (1993) 449–454.